New control architecture for high performance autopilot

Article · January 2011

CITATIONS
0

READS
418

2 authors:

I. Rusnak
Rafael Advanced Defense Systems
166 PUBLICATIONS **1,518** CITATIONS
SEE PROFILE

Haim Weiss
56 PUBLICATIONS **1,239** CITATIONS
SEE PROFILE

NEW CONTROL ARCHITECTURE FOR HIGH PERFORMANCE AUTOPILOT

Ilan Rusnak and Haim Weiss
RAFAEL, P. O. Box 2250, Haifa, Israel.

ABSTRACT

Missile autopilots are designed to guarantee stability and performance throughout the flight envelope. The stability and performance are conflicting objectives. The final design is a compromise between stability margins and autopilot agility. In this paper novel control architecture for high performance autopilots is presented that has the potential to resolve the conflict between robust stability and robust performance. This new architecture is motivated by control architectures generated from the model reference tracking problem. These architectures are widely used in high performance motion control systems. In the paper the theory of linear quadratic tracking is used to develop the proposed control architectures and structures. The potential of improvement in performance of these architectures is demonstrated via appropriate simulations. This demonstrates the advantage of the proposed autopilot control architecture.

1. INTRODUCTION

Missile autopilots are designed to guarantee stability and performance throughout the flight envelope. The stability and performance are conflicting objectives. The commonly used control architectures do not enable to separate the stability objective from the performance objective. The final design is a compromise between stability margins and autopilot agility. The high gain required for high performance leads to inadequate gain and phase margins.

Proper architecture can resolve the conflict between stability and performance. In this paper novel control architecture for high performance autopilots is introduced. This new architecture is motivated by control architectures that are widely used in high performance motion control systems [1, pp. 80, 347]. The proposed control architecture enables the separation of the two objectives, the stability and the performance, and considers them as two separate issues.

The main purpose of this paper is to introduce the model following paradigm as a vital tool for high performance autopilots.

Asseo [2] applied optimal control to the perfect model following problem, derived the solution for Type-Zero (no integrators in open loop) and Type-One (one integrator in open loop on each state), and implemented the concept on aircraft autopilot model.

The proposed architecture uses the architecture generating property of the Linear Quadratic Regulator-LQR and the Linear Quadratic Tracking-LQT criteria [3, 4]. This property had been used to show those problems for which the PID controller is the optimal controller [5]. Further it had been used to derive the generalized PID controller for high order plants [6], and to devise the structure of the controller for deterministic [7] and stochastic [8] motion control systems.

Mracek and Ridgley [9] used the architecture generating property of the LQR criterion to derive architectures (set up of the blocks) and structures (content of the blocks) for the three loop autopilot. The motivation behind this paper is to generalize this outcome and to design control architecture based on the LQT solution. In this approach a reference system generates the desired state trajectory that the system is required to follow.

In our case the reference model is the nominal design of the three loop autopilot. Such a reference model guarantees that unrequired excessive control will not be applied to the plant. This way the controller is designed to correct only the deviations from the nominal response.

The application of the LQT methodology, which widely and successfully used in high performance motion control, has the potential of implementing high performance autopilots.

The paper deals with "Type-Zero" model following (proportional feedback) and "Type-One" model following (proportional + integral feedback). Implementation of Type-N control is the issue of further research.

The performance of all the discussed architectures and structures is demonstrated via appropriate simulations. This clearly demonstrates the advantage of the proposed autopilot control architecture.

2. STATEMENT OF THE PROBLEM

In the existing design approaches of autopilots usually robust stability means conservative performance and high performance means reduced stability margins.

The novel proposed architecture enables the separation of the robust stability and robust performance problem into two loosely coupled problems. To be more specific: the presented architecture reduces the coupling between the performance and robustness, thus greatly eases the design. The robust stability problem is implemented by the design of the closed loop controllers. The robust performance is implemented by feed forward signals generated by the reference trajectory.

3. OPTIMAL MODEL REFERENCE TRACKING SYSTEMS

This section reviews the optimal model reference tracking problem [2, 10] and the generalized PI controllers [5-8]. This problem motivates the existing control architectures that are widely used in the motion control industry [1]. Further it derives a specific solution for Type-Zero and Type-One control criteria under the assumption that the reference model represents the actual behaviour of the autopilot without uncertainties to a reasonable degree and achieves the required performance.

3.1 Type-Zero Optimal Tracking Problem

We assume the n-th order multi-input multi-output system

$$\begin{aligned} &\dot{x} = Ax + Bu + \Gamma w, \quad x(t_o) = x_o, \\ &y = Cx \end{aligned} \tag{1}$$

where $x \in R^n$ is the state; $u \in R^m$ is the input, $w \in R^\mu$ is a disturbance and $y \in R^p$ is the measured output; $A \in R^{nxn}$, $B \in R^{nxm}$, $\Gamma \in R^{nx\mu}$ and $C \in R^{pxn}$ are matrices with proper dimensions. The initial condition x_o is a zero mean random vector.
The reference trajectory generator is described by

$$\begin{aligned} \dot{x}_r &= A_r x_r + \Gamma_r w_r, \quad x_r(t_o) = x_{ro}, \\ y_r &= C_r x_r \end{aligned} \tag{2}$$

where $x_r \in R^v$ is the state; $w_r \in R^m$ is the reference trajectory generator input and $y_r \in R^p$ is the reference output; $A_r \in R^{vxv}$, $\Gamma_r \in R^{v \times m}$ and $C_r \in R^{pxv}$. The reference trajectory generator input, w_r, is a zero mean stochastic process. The initial condition x_{ro} is a zero mean random vector.
The Type-Zero tracking objective is

$$\begin{aligned} J = \tfrac{1}{2} E\{ & (y(t_f) - y_r(t_f))^T G_1 (y(t_f) - y_r(t_f)) \\ & + \int_{t_o}^{t_f} [y(t) - y_r(t))^T Q_1 (y(t) - y_r(t)) + u(t)^T R u(t)] dt \} \end{aligned} \tag{3}$$

The expectation is taken with respect to the reference trajectory generator input, w_r, the plant disturbance, w, and the initial conditions. The optimal tracking problem [10] is to find an admissible input u(t) such that the tracking objective (3) is minimized subject to the dynamic constraints (1, 2).

3.2 Type-One Optimal Tracking Problem

We assume the n-th order multi-input multi-output system (1). The reference trajectory generator is (2). The integral action is introduced into the control in order to "force" zero tracking errors for polynomial inputs, and to attenuate constant or polynomial disturbances. This is done by introducing an auxiliary variable, the integral of the tracking error

$$\dot{\eta} = e = y - y_r \tag{4}$$

The Type-One tracking objective is

$$\begin{aligned} J = \tfrac{1}{2} \{ & (y(t_f) - y_r(t_f))^T G_1 (y(t_f) - y_r(t_f)) + \eta(t_f)^T G_2 \eta(t_f) \\ & + \int_{t_o}^{t_f} [y(t) - y_r(t))^T Q_1 (y(t) - y_r(t)) + \eta(t)^T Q_2 \eta(t) + u(t)^T R u(t)] dt \} \end{aligned} \tag{5}$$

The optimal tracking problem [10] is to find an admissible input u(t) such that the tracking objective (5) is minimized subject to the dynamic constraints (1, 2, 4).

3.3 Solution of the Type-Zero Tracking Problem

In order to solve the Stochastic Optimal Tracking Problem we augment the state variables to the form [10]

$$\xi = \begin{bmatrix} x \\ x_r \end{bmatrix}, \xi_o = \begin{bmatrix} x_o \\ x_{ro} \end{bmatrix} \quad \overline{A} = \begin{bmatrix} A & 0 \\ 0 & A_r \end{bmatrix}, \quad \overline{B} = \begin{bmatrix} B \\ 0 \end{bmatrix}, \quad \overline{C} = \begin{bmatrix} C & -C_r \end{bmatrix}, \quad \overline{w} = \begin{bmatrix} w \\ w_r \end{bmatrix}, \tag{6}$$

Then the minimization of (3) subject to (1, 2) is replaced by the minimization of

$$J = \tfrac{1}{2} E\{\xi(t_f)^T G \xi(t_f) + \int_{t_o}^{t_f} [\xi(t)^T Q \xi(t) + u(t)^T R u(t)] dt\} \tag{7}$$

subject to

$$\dot{\xi} = \overline{A}\xi + \overline{B}u + \overline{w}_r, \bar{x}(t_o) = \bar{x}_o \tag{8}$$

where

$Q = \overline{C}^T Q_1 \overline{C}$, $G = \overline{C}^T G_1 \overline{C}$.

The problem above is the stochastic linear optimal regulator problem defined and solved in [10, 11]. The solution is

$$\begin{aligned} u &= -R^{-1}\overline{B}^T P \xi \\ -\dot{P} &= P\overline{A} + \overline{A}^T P + Q - P\overline{B}R^{-1}\overline{B}^T P, P(t_f) = G, \end{aligned} \tag{9}$$

Notice that the solution is not affected by $\overline{w}$. This is due to the assumption that it is a zero mean stochastic process. If we write P={[P_{ij}]; i,j=1,2}, then

$$u = -R^{-1}\begin{bmatrix} B^T P_{11} & B^T P_{12} \end{bmatrix} \begin{bmatrix} x \\ x_r \end{bmatrix} \tag{10}$$

The LQT induced architecture is presented in Figure 1.

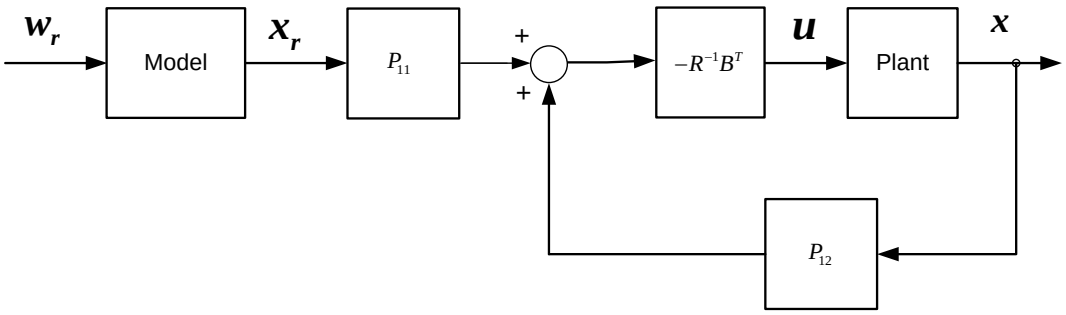

Figure 1: The Type-Zero tracking architecture.

3.4 Specific solution - The Generalized P Controller

For the case n=ν, $A=A_r$, $\Gamma = \Gamma_r$ and $C = C_r = I$, i.e. the reference trajectory generator is identical to the plant, it can be shown that $P_{12} = -P_{11}$. Then

$$u = -R^{-1}\begin{bmatrix} B^T P_{11} & B^T P_{12} \end{bmatrix} \begin{bmatrix} x \\ x_r \end{bmatrix} = -R^{-1}B^T P_{11}[x - x_r] = K_1 e \tag{11}$$

Where

$$K_1 = -R^{-1}B^T P_{11}. \tag{12}$$

Figure 2 presents the Type-Zero tracking architecture and structure associated with (11).

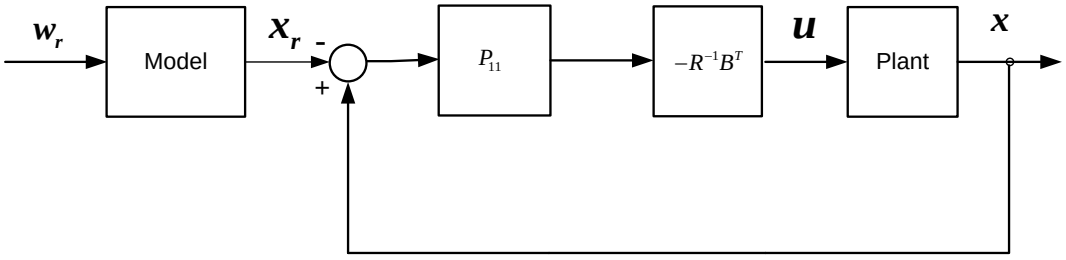

Figure 2: The Type-Zero tracking architecture and structure.

3.5 Solution of the Type-One Tracking Problem - The generalized PI controller

In order to solve the Type-One Optimal Tracking Problem we augment the state variables to the form [10]

$$\bar{x}=\begin{bmatrix} x \\ \eta \\ x_r \end{bmatrix},\ \bar{A}=\begin{bmatrix} A & 0 & 0 \\ C & 0 & -C_r \\ 0 & 0 & A_r \end{bmatrix},\quad \bar{B}=\begin{bmatrix} B \\ 0 \\ 0 \end{bmatrix},\ \bar{C}=\begin{bmatrix} C & 0 & -C_r \end{bmatrix}, \tag{13}$$

Then the minimization of (5) subject to (1, 2, 4) is replaced by the minimization of

$$J=\tfrac{1}{2}\{x(t_f)^T Gx(t_f)+\int_{t_o}^{t_f}[x(t)^T Qx(t)+u(t)^T Ru(t)]dt\} \tag{14}$$

subject to

$$\dot{\bar{x}}=\bar{A}\bar{x}+\bar{B}u \tag{15}$$

where

$$Q=\bar{C}^T Q_1\bar{C}+\begin{bmatrix} 0 \\ 1 \\ 0 \end{bmatrix}Q_2\begin{bmatrix} 0 & 1 & 0 \end{bmatrix} \tag{16a}$$

$$G=\bar{C}^T G_1\bar{C}+\begin{bmatrix} 0 \\ 1 \\ 0 \end{bmatrix}G_2\begin{bmatrix} 0 & 1 & 0 \end{bmatrix} \tag{16b}$$

Observe that the solution is not affected by w_r.

Also notice that in the solution we assumed that $w_r=0$ or for the stochastic formulation that $E[w_r]=0$.

The solution is [10, 11]

$$\begin{aligned} u&=-R^{-1}\bar{B}^T P\bar{x} \\ -\dot{P}&=P\bar{A}+\bar{A}^T P+Q-P\bar{B}R^{-1}\bar{B}^T P, P(t_f)=G, \end{aligned} \tag{17}$$

If we write P={[P_{ij}]; i,j=1,2,3}, then

$$u = -R^{-1} \quad [\, B^T P_{11} \;\; B^T P_{12} \;\; B^T P_{13} \,] \begin{bmatrix} x \\ \eta \\ x_r \end{bmatrix}, \tag{18}$$

Figure 3 presents the Type-One tracking architecture and structure.

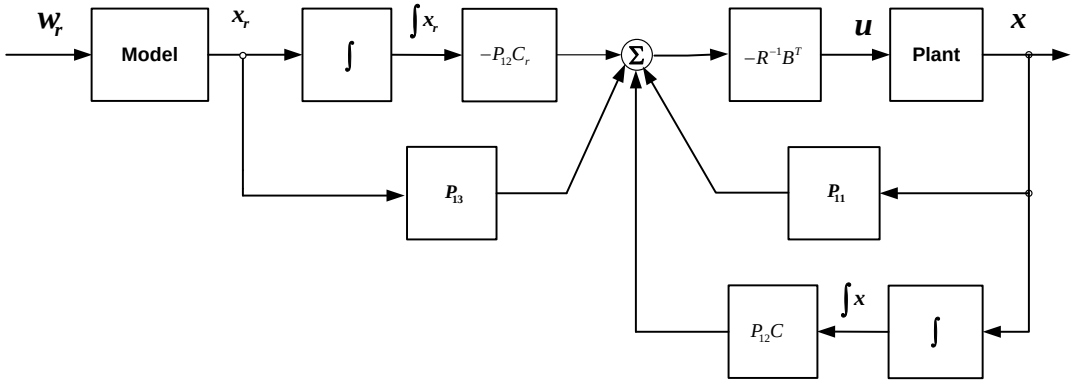

Figure 3: The Type-One tracking architecture and structure.

3.6 Specific solution - The General PI Controller

Consider the case $A=A_r$, $C=C_r = I$ and $\Gamma = \Gamma_r$, i.e. the reference trajectory generator is identical to the plant. In this case it can be shown that $P_{13} = -P_{11}$. (See Appendix A for 1st order system).

Since $P_{13} = -P_{11}$ the control u can be expressed as

$$u = -R^{-1}\begin{bmatrix} B^T P_{11} & B^T P_{12} & B^T P_{13} \end{bmatrix} \begin{bmatrix} x \\ \eta \\ x_r \end{bmatrix} = K_1 e + K_2 \int e dt \tag{19}$$

where

$$K_1 = -R^{-1}\, B^T P_{11}, \qquad K_2 = R^{-1}\, B^T P_{12}. \tag{20}$$

Figure 4 presents the Type-One tracking architecture and structure. It is shown in [5-8] that this is the generalized PI controller.

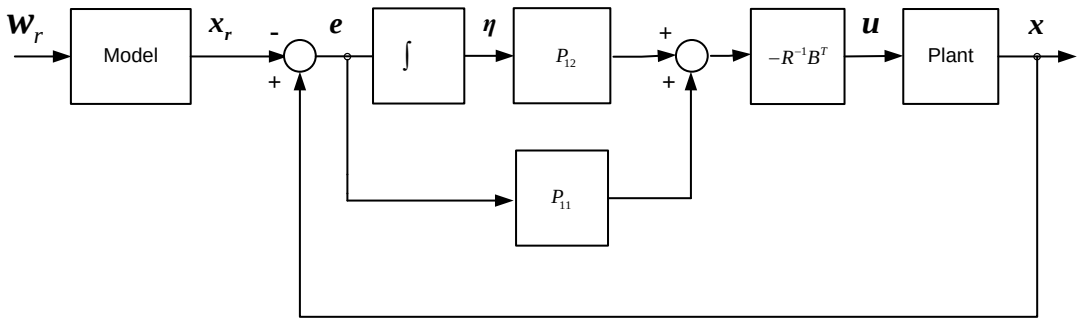

Figure 4: The Type-One tracking architecture and structure.

4. THE EXISTING THREE LOOP AUTOPILOT

Many missiles use a three loop lateral autopilot, see [12], as shown in Figure 5. More information on this architecture can be found in [13] and [14].
The three loops are the synthetic stability loop, the accelerometer feedback loop, and the rate loop. The major components of the flight control system include the airframe, the aerodynamic control surfaces, the actuator, the rate gyro, and the accelerometer. The rate loop is the wide band loop in the system and structural vibrations are most evident in that loop.

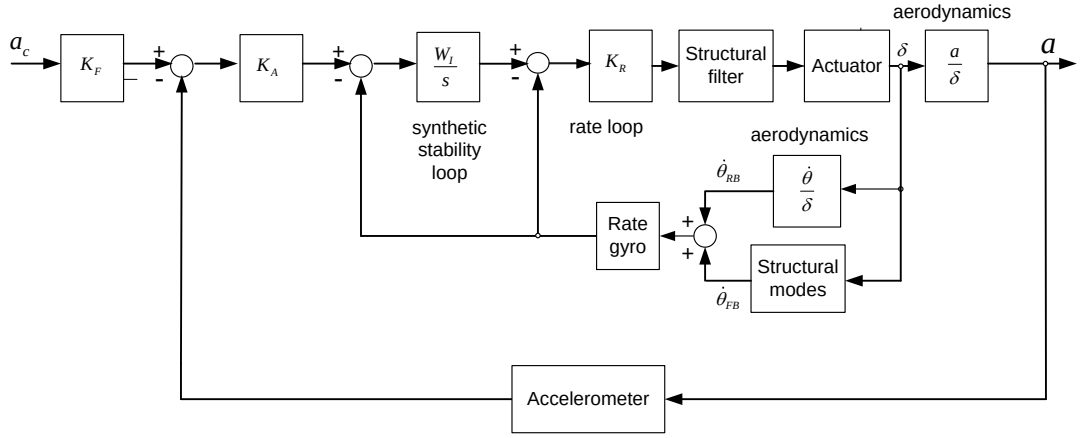

Figure 5: Three loop pitch/yaw autopilot block diagram.

The design scheme presented in Fig. 5 is based on the following assumptions: The Inertial Measuring Unit (IMU) is located in the body center of gravity. Each of the modal transfer functions is in parallel with the rigid body aerodynamic transfer function. The gyro senses the flexible body motions in addition to the rigid body motions. The accelerometer also measures vibration of the body; however this additional path has much less effect on system response and therefore has been neglected. The accelerometer transfer function is assumed to be 1, i.e., ideal accelerometer.

5. THE REFERENCE MODEL.

The novel architecture is composed from a reference model and feedforward as further detailed in the next section. The reference model: (i) imitates the behaviour of the actual autopilot without uncertainties; and (ii) achieves the required performance. Figure 5 presents the architecture of the three loops Type-Zero autopilot of [12]. Figure 6 presents the block diagram of the reference model.

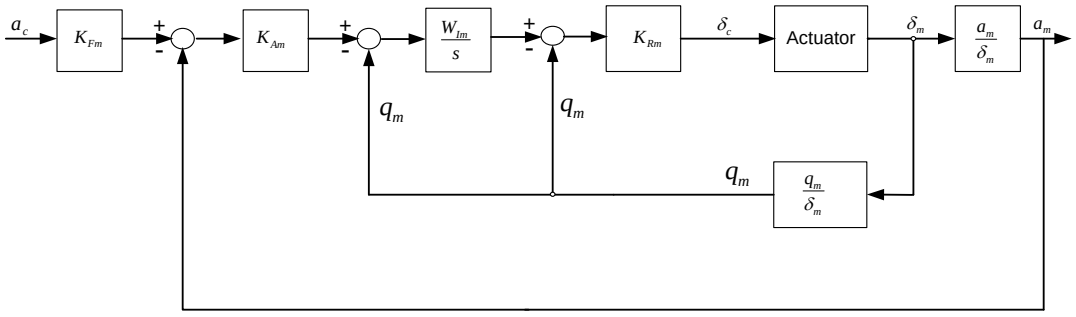

Figure 6: Type-Zero three loops reference model autopilot.

Formally, it is a model of the missile's autopilot without the structural-resonant modes and the structural filters, with ideal gyro and accelerometer, servo and nominal aerodynamics.
The reference model is in the full hands of the designer. The designer is free to require any response time and the stability is inherently incorporated in the reference model design. The reference model is implemented in the software of the controller.

Notice: The reference trajectory generator can be "any" stable dynamic system. There are no uncertainties, and there is no concern about robustness as it is implemented in the controller software.

6. THE NEW CONTROL ARCHITECTURE – MODEL REFERENCE TRACKING AUTOPILOT

Conceptual architectures are presented in Figures 7 and 8 for Type-Zero and Type-One control, respectively. The integral action on the acceleration and body rate errors may be seen in Figure 8. A heuristic explanation of the operation is as follows: The commanded acceleration, a_c, is applied to the model input. The respective states of the reference model are fed forward to the respective blocks' inputs of the autopilot. The real missile tracks the feedforward signals generated by the reference model and the feedback takes care of any miss-match between the reference model and the actual missile including initial condition. Thus, errors in the missile's autopilot will converge to small values.
In this way the controllers in the missile's autopilot should be designed for robust stability and the reference model together with the feedforward take care of the performance.
The proposed control architecture also takes care of following issues: (i) Non-linearities in the real missile are linearized by the feedback; and (ii) Limitations and constraints on the real missile can be incorporated into the reference model to prevent the missile "hit" them. Such limitations are maximal fin angle, maximal fins rate, maximal acceleration, maximal angle of attack, ...
It should be emphasized that in this architecture, although feedforward is implemented, no differentiation is involved, and the noise is not amplified by the feedforward action.

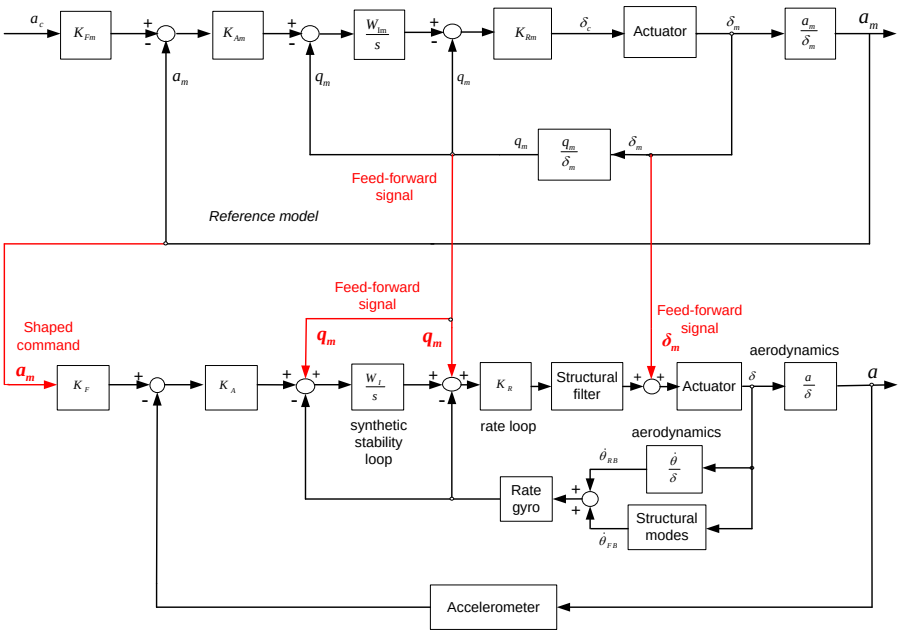

Figure 7: Type-Zero model reference tracking autopilot.

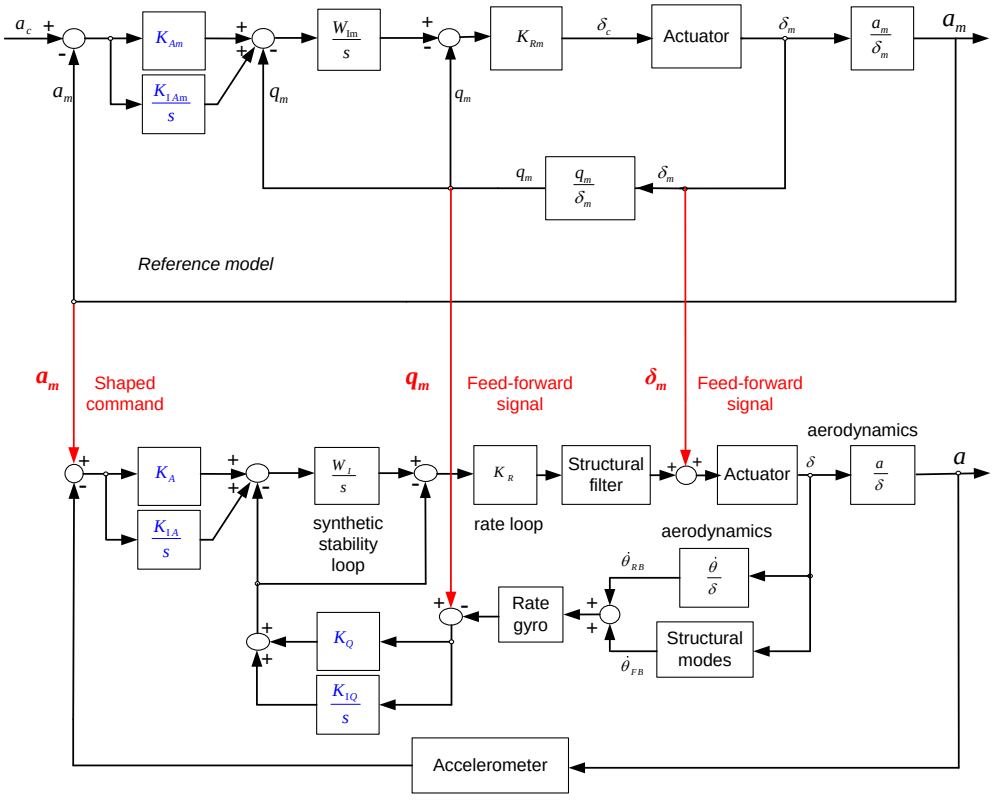

Figure 8: Type-One model reference tracking autopilot.

7. EXISTING THREE LOOP AUTOPILOT DATA AND PERFORMANCE

The autopilot parameters follow [12]. The relevant gains and transfer functions follow the notation of Figure 5. The respective Simulink® Program that produced these results is presented in appendix B. The aerodynamic gain reduction had been emulated by reduction of the DC gain of the actuator, a gain of 1 in the block diagram of appendix B.
Controller gains:

$$K_F = 1/0.7387,\ K_A = 0.0018208,\ W_I = 15.82481,\ K_R = 0.33835/2$$

Notice that the gain K_R had been reduced by 6dB with respect to [12] to achieve larger gain margin.

Aerodynamic transfer functions:

$$\frac{\dot{\theta}}{\delta} = \frac{0.6477(0.676s+1)}{(s/22.4)^2 + 2\times(0.052/22.4)s+1}$$

$$\frac{a}{\delta} = \frac{-1116.5(-0.00081s^2 + 0.0010546s+1)}{(s/22.4)^2 + 2\times(0.052/22.4)s+1}$$

Rate gyro transfer function:

$$\frac{\dot{\theta}_G}{\dot{\theta}} = \frac{1}{(s/500)^2 + 2\times(0.65/500)s+1}$$

Actuator transfer function:

$$\frac{\delta}{\delta_c} = \frac{1}{(s/250)^2 + 2\times(0.7/250)s+1}$$

The transfer functions from control surface angle to body rate for each of the flexible modes are:
1st structural mode:

$$\frac{\dot{\theta}_{FB_1}}{\delta} = \frac{0.00134[(s/345)^2+1]s}{(s/259)^2 + 2\times(0.015/259)s+1}$$

2st structural mode:

$$\frac{\dot{\theta}_{FB_2}}{\delta} = \frac{0.000664[(s/255)^2+1]s}{(s/699)^2 + 2\times(0.022/699)s+1}$$

Structural filters transfer functions:

$$F_1(s) = \frac{(s/259)^2+1}{(s/259)^2 + 2\times(0.7/259)s+1}$$

$$F_2(s) = \frac{(s/699)^2+1}{(s/699)^2 + 2\times(0.7/699)s+1}$$

Typical step responses of the design described in [12] are depicted in Figure 9. The step responses include the nominal case and cases where the gain of the transfer function δ/δ_c is different from the nominal by ±3dB. The response demonstrates the performance and robustness of the design as presented in [12]. The response is clearly non-minimum phase with time constant of about 0.3 sec and with small amplitude oscillations.

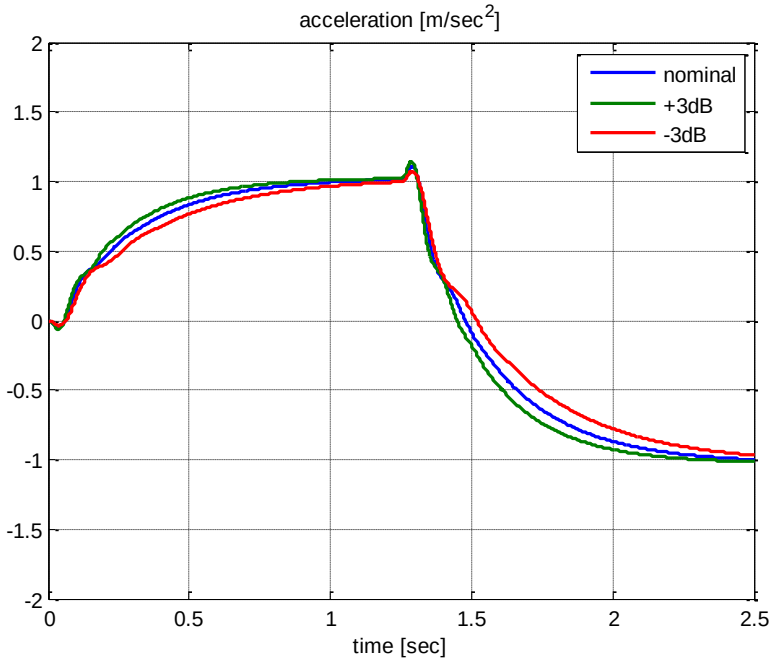

Figure 9: Step response of the existing three loop autopilot design in the nominal case and where the gain of δ/δ_c is different from the nominal by ±3dB.

8. TYPE-ZERO ARCHITECTURE PERFORMANCE

Figure 10 presents the nominal response and the acceleration tracking error of the novel Type-Zero architecture autopilot. The faster response may be clearly seen. The respective Simulink® Program that produced these results is presented in appendix C. The tracking error for unit step is less than 10%. The response time constant had been reduced from 0.3sec to 0.1 sec. No special dedicated procedure had been applied in the design of the reference model or the autopilot. Thus it might be expected that such design procedure can further reduce the tracking error. In spite of it the time response improvement is significant.

Figure 11 presents the response and the acceleration tracking error of the autopilot of the novel Type-Zero architecture autopilot for 3dB reduction of the aerodynamic gain that had been emulated by the reduction of δ/δ_c gain. The time response is fast but the nonzero steady state error is clearly seen. It is the result as the Type-Zero control is applied.

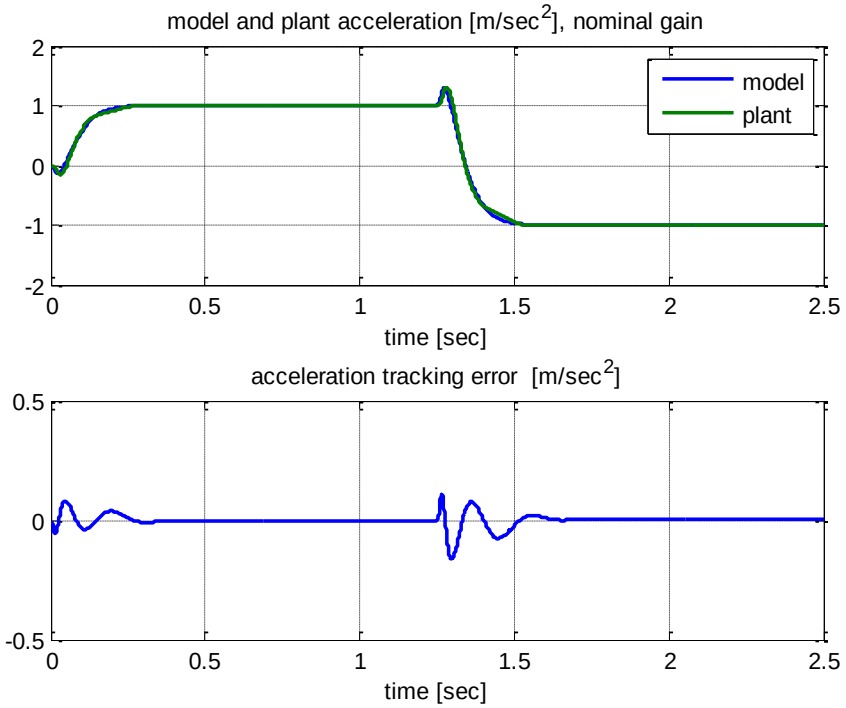

Figure 10: Nominal response of the novel Type-Zero architecture autopilot.

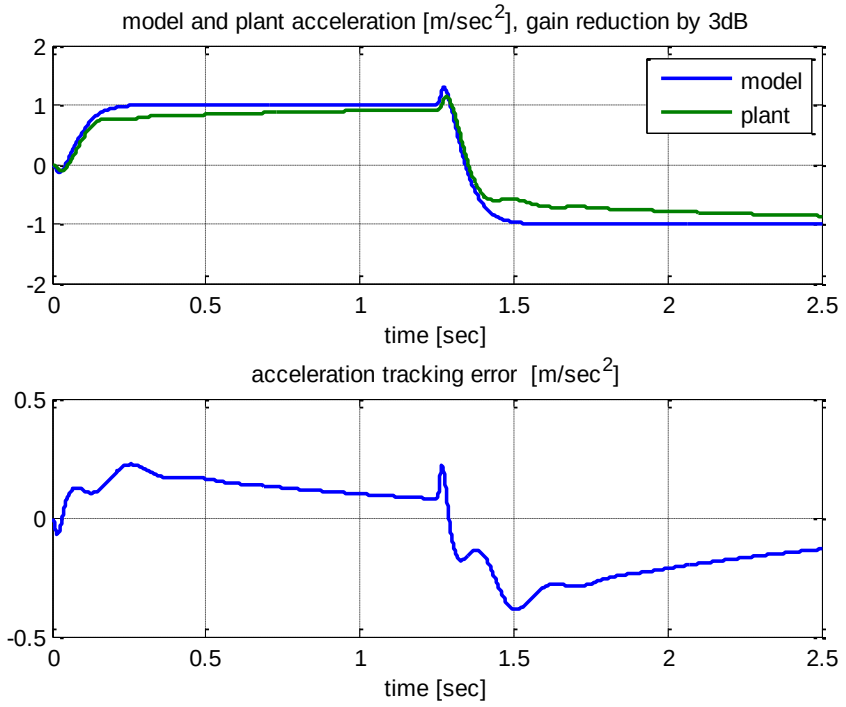

Figure 11: The response and the acceleration tracking error of the novel Type-Zero architecture autopilot for 3dB reduction of the aerodynamic gain.

9. TYPE-ONE ARCHITECTURE PERFORMANCE

Figure 12 presents the nominal response and the acceleration tracking error of the novel Type-One architecture autopilot. The faster response may be clearly seen. The respective Simulink® Program that produced these results is presented in appendix D. The tracking error for unit step is about than 2%. The steady state error is now zero due to the Type-One control (integral action) in both the model and the autopilot itself. The response time constant is 0.15 sec. The inclusion of the integral action is responsible to the slightly slower time response.
No special dedicated procedure had been applied in the design of the reference model or the autopilot. Thus it might be expected that such design procedure can further reduce the tracking error. In spite of it the time response improvement is significant.
.

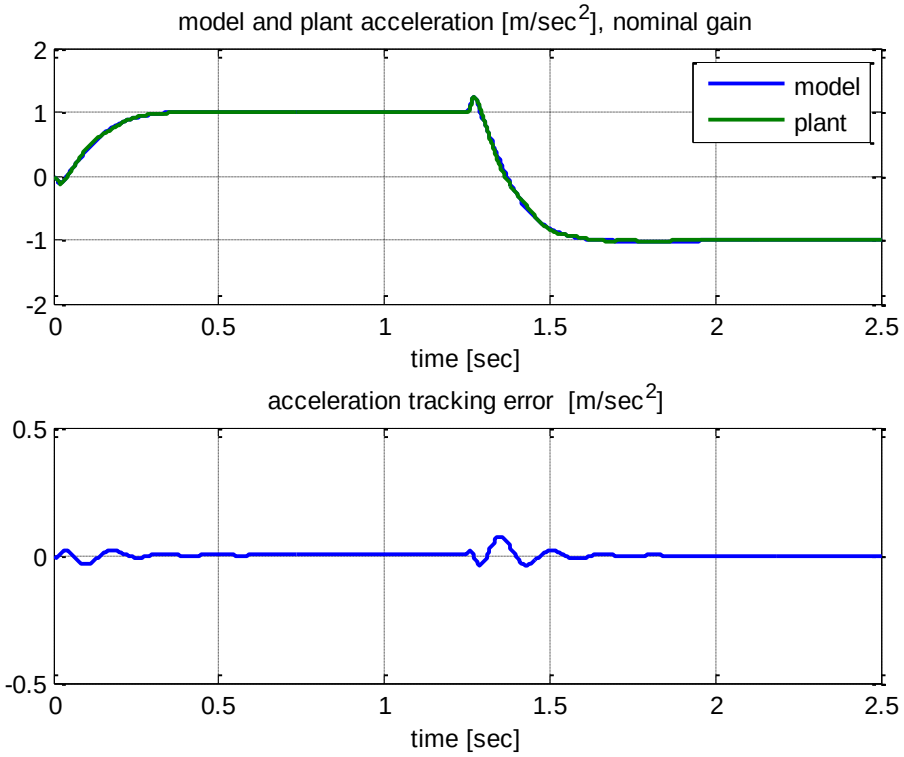

Figure 12: The nominal response and the acceleration tracking error of the novel Type-One architecture autopilot.

Figure 13 presents the response and the acceleration tracking error of the autopilot of the novel Type-Zero architecture autopilot for 3dB reduction of the aerodynamic gain that had been emulated by the reduction of δ/δ_c gain.

Figure 14 presents the response and the acceleration tracking error of the novel Type-one architecture autopilot for 3dB reduction of the aerodynamic gain without integral action on the body rate error. The aerodynamic gain had been emulated by the reduction of δ/δ_c gain. By comparison of figure 13 to 14 one can see the improving effect of the integral action on the body rate error. It reduces the acceleration tracking error.

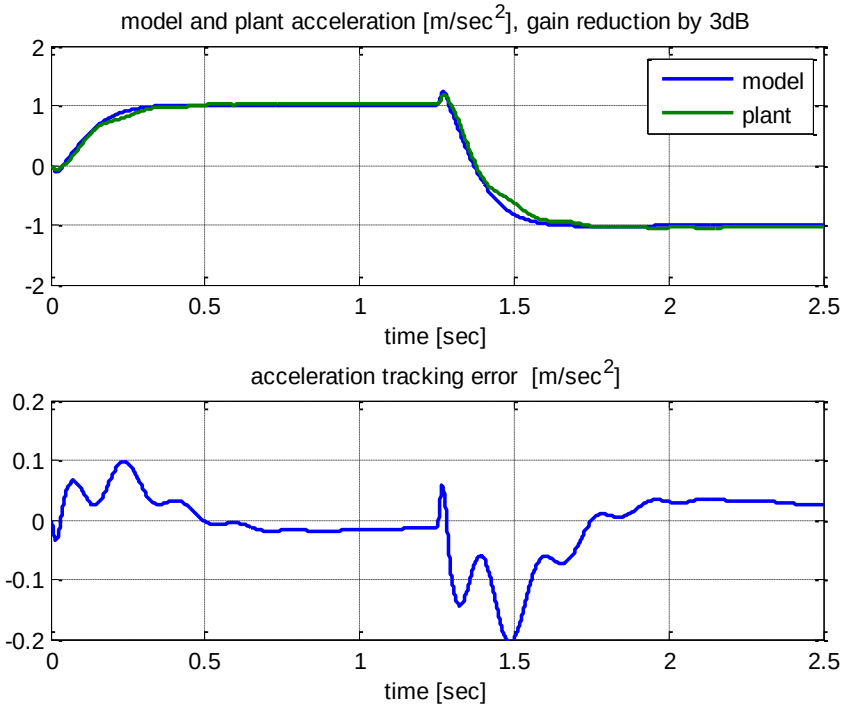

Figure 13: The response and the acceleration tracking error of the novel Type-one architecture autopilot for 3dB reduction of the aerodynamic gain.

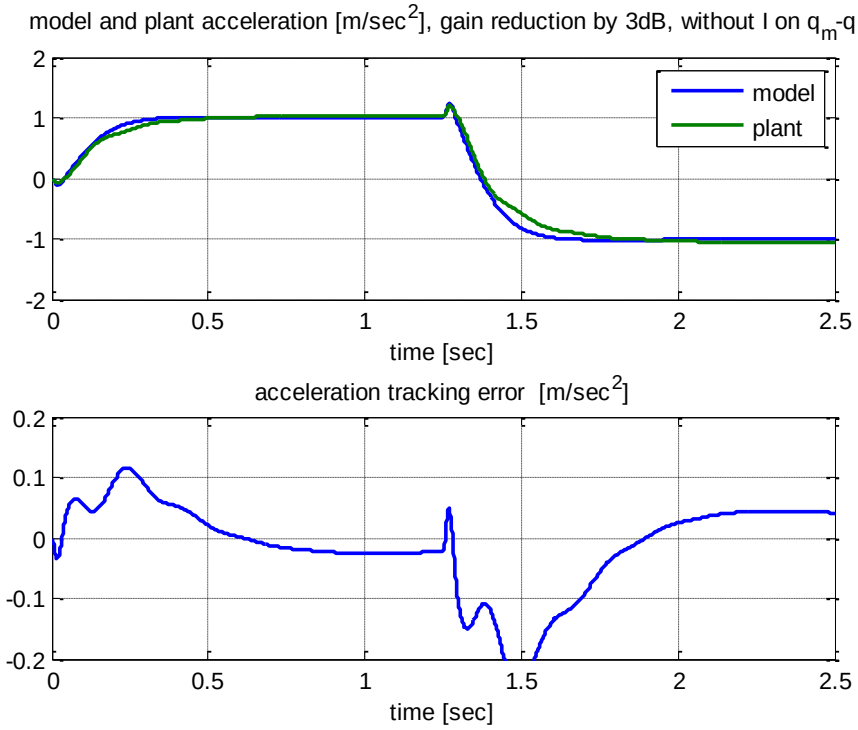

Figure 14: The response and the acceleration tracking error of the novel Type-one architecture autopilot for 3dB reduction of the aerodynamic gain without integral action on the body rate error.

10. DISCUSSION

10.1 Separation of the robust stability and performance

The novel proposed architecture enables the separation of the robust stability and robust performance problem into two problems. To be more specific: The presented architecture introduces a degree of decoupling between the performance and robustness, thus greatly eases the design. The robust stability problem is implemented by the design of the closed loop controllers. The robust performance is implemented by the feed forward signals produced by the reference trajectory generator.

10.2 The importance of smooth repeatable response

For high performance missile Optimal Guidance Laws should be implemented [13, 15, 16]. These guidance laws optimize simultaneously the miss distance and the energy expenditure (induces drag) of the missile. The optimal guidance laws require good knowledge of the missile's parameters namely, the autopilots' transfer function to achieve the desired performance. Thus first order approximation is insufficient. Untreated miss-match of the guidance law to the actual transfer function of the autopilot may lead to unstable guidance loop [17]. Such miss-match causes an increase of the miss distance, the induced drag and the internal energy expenditure (smaller performance envelope).

11. CONCLUSIONS

Novel control architecture for robust stability and high performance autopilots has been presented. This control architecture is motivated by the model following control paradigm. It enables partial decoupling of the robust stability and performance objectives. The potential of improvement in performance of all the architectures is demonstrated via appropriate simulations.

12. REFERENCES

[1] W, Leonhard, *Control of Electrical Drives*, Springer-Verlag, 1996.

[2] S. J. Asseo, "Application of Optimal Control to Perfect Model Following", *Journal of Aircraft*, Vol. 7, No. 4, July-August 1970, pp.308-313.

[3] I. Rusnak, "Control and Feedback Organization – Review and Terminology," Proc. of the *24th IEEE Conference of Electrical and Electronics Engineers in Israel*, Eilat, Israel, November 15-17, 2006.

[4] I. Rusnak, "Control Organization – Survey and Application," Proc. of the *9th Biennial ASME Conference on Engineering Systems Design and Analysis*, ESDA 2008, 7-9 July, Haifa, Israel.

[5] I. Rusnak, "The Optimality of PID Controllers," Proc. of the *9th Mediterranean Electro-technical Conference*, MELECON '98, May 18-20, 1998, Tel-Aviv, Israel.

[6] I. Rusnak, "Generalized PID Controllers," Proc. of the *7th IEEE Mediterranean Conference on Control & Automation*, MED 99, 28-29 June 1999, Haifa, Israel.

[7] I. Rusnak, "The Generalized PID Controller and its Application to Control of Ultrasonic and Electric Motors," *PID' 2000, IFAC Workshop on Digital Control, Past, Present and Future of PID Control*, Terrassa, Spain, 5-7 April, 2000.

[8] I. Rusnak, "Generalized PID Controller for Stochastic Systems," Proc. of the *21st Convention of IEEE in Israel*, April 11-12, 2000, Tel-Aviv, Israel. (Invited paper).

[9] C. P. Mracek and D. B. Ridgley, "Connections Between Optimal Control and Classical Topologies, Proc. of the *AIAA Guidance , Navigation and Control Conference*, 15-18 August 2005, San Francisco, CA, USA. 2005-6381.

[10] H. Kwakernaak and R. Sivan, *Linear Optimal Control*, John Wiley & Sons, Inc., 1972.

[11] A. E. Bryson and Y.C. Ho, *Applied Optimal Control*, John Wiley & Sons, 1964.

[12] F. W. Nesline and M. L. Nesline, "Phase vs. Gain Stabilization of Structural Feedback Oscillations in Homing Missile Autopilots, Proc. of the *American Control Conference*, 19-21 June 1985, pp. 323-329.

[13] R. Aggarwal and D. Boudreau, "An Implementable High-Order Guidance Law for Homing Missiles, Proc. of the *34th Conf. on Decision and Con*trol, New Orleans, LA, USA, December 1995, Vol. 2 pp. 1965-1966.

[14] C. P. Mracek, and D. B. Ridgley, "Missile Longitudinal Autopilots: Comparison of Multiple Three Loop Topologies", Proc. of the *AIAA Guidance, Navigation and Control Conference*, 15-18 August 2005, San Francisco, CA, USA. 2005-6380.

[15] I. Rusnak, and L. Meir, "Modern Guidance Law for High Order Autopilot", *Journal of Guidance, Control and Dynamics*, Vol. 14, No. 5, September-October 1991, pp. 1056-1058.

[16] I. Rusnak, and L. Meir, "Optimal Guidance for High Order and Acceleration Constrained Missile", *Journal of Guidance, Control and Dynamics*, Vol. 14, No. 3, May - June 1991, pp. 589-596.

[17] H. Weiss and G. Hexner, "Stability of Modern Guidance Laws with Model Mismatch," Proc. of the *American Control Conference*, Boston, Massachusetts, June 30 July 2, 2004, pp. 3634-3639.

Appendix A: The PI controller for first order system

If $A = A_r = 0$, $C = C_r = 1$ and $B = B_r = 1$, i.e. one integrator, then from (17)

$$0 = - P_{12} - P_{12} + Q_1 - P_{11}R^{-1}P_{11} \quad \text{(A.1a)}$$

$$0 = - P_{22} - P_{11}R^{-1}P_{12} \quad \text{(A1.b)}$$

$$0 = P_{12} - P_{23} - Q_1 - P_{11}R^{-1}P_{13} \quad \text{(A.1c)}$$

$$0 = Q_2 - P_{12}R^{-1}P_{12} \quad \text{(A.1d)}$$

$$0 = P_{22} - P_{12}R^{-1}P_{13} \quad \text{(A.1e)}$$

$$0 = P_{23} + P_{23} + Q_1 - P_{13}R^{-1}P_{13} \quad \text{(A.1f)}$$

from (A.1d)

$$P_{12} = -\sqrt{Q_2 R} \quad \text{(we select the negative root)} \quad \text{(A.2)}$$

from (A.1a) and (A.2)

$$P_{11} = -\sqrt{R(Q_1 - 2P_{12})} = R\sqrt{\frac{Q_1}{R} + 2\sqrt{\frac{Q_2}{R}}} \quad \text{(A.3)}$$

from (A.1b)

$$P_{22} = -\frac{P_{12}P_{11}}{R} \quad \text{(A.4)}$$

from (A.1e) and (A.4)

$$P_{13} = \frac{P_{22}R}{P_{12}} = -P_{11}. \quad \text{(A.5)}$$

This means, by the use of (18), that

$$\begin{aligned} u &= -\frac{1}{R}\begin{bmatrix} P_{11} & P_{12} & -P_{11} \end{bmatrix}\begin{bmatrix} x \\ \eta \\ x_r \end{bmatrix} = -\begin{bmatrix} k_1 & k_2 & -k_1 \end{bmatrix}\begin{bmatrix} x \\ \eta \\ x_r \end{bmatrix} \\ &= k_1(x - x_r) + k_2\eta = k_1 e + k_2 \int e dt \end{aligned} \quad \text{(A.6)}$$

This is the PI controller.

Appendix B: Three loop autopilot [12] (Raytheon_ap_1a.mdl)

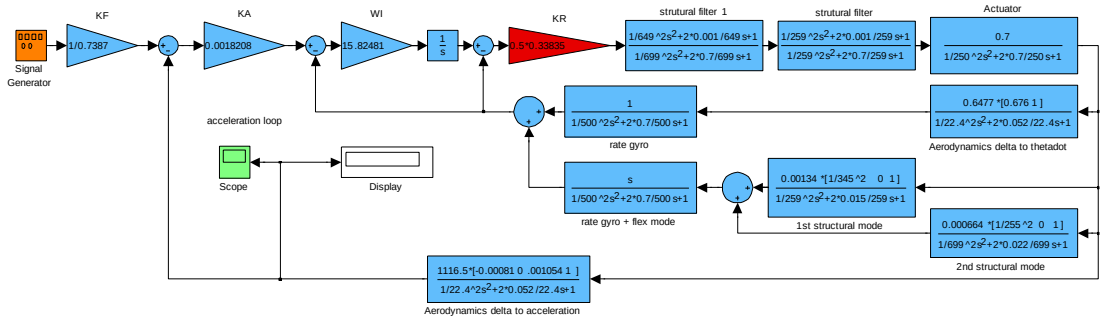

Appendix C: Type-Zero model reference tracking autopilot (IACAS_architecture_2a.mdl)

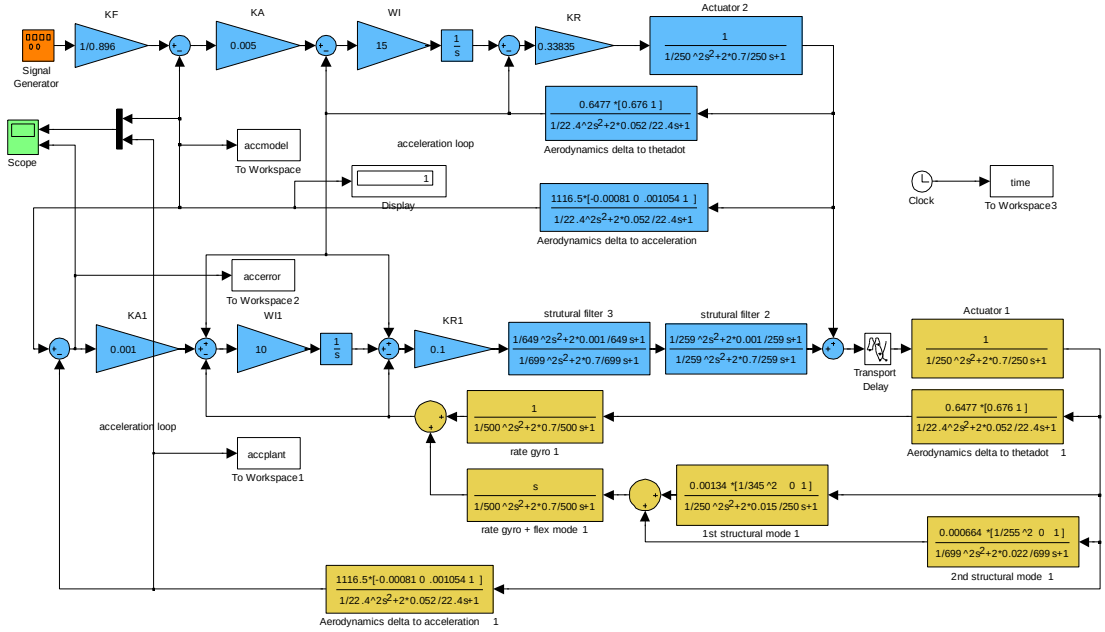

Appendix D: Type-One model reference tracking autopilot (IACAS_architecture_4x.mdl)